Local Structure in a Tryptic Fragment of Performic Acid Oxidized Ribonuclease A Corresponding to a Proposed Polypeptide Chain-Folding Initiation Site Detected by Tyrosine Fluorescence Lifetime and Proton Magnetic Resonance Measurements†

Elisha Haas

Department of Life Sciences, Bar-Ilan University, Ramat-Gan 52100, Israel, and Biophysics and Chemical Physics Department, Weizmann Institute, Rehovot 76100, Israel

Gaetano T. Montelione, Charles A. McWherter, and Harold A. Scheraga*

Baker Laboratory of Chemistry, Cornell University, Ithaca, New York 14853-1301

Received May 20, 1986; Revised Manuscript Received October 13, 1986

ABSTRACT: The effects of proline and X–Pro peptide bond conformations on the fluorescence properties of tyrosine in peptides corresponding to parts of a proposed chain-folding initiation site in bovine pancreatic ribonuclease A are examined by time-resolved and steady-state fluorescence spectroscopy. In peptides with Tyr-Pro sequences, the conformational constraints of proline on a preceding residue result in significant fluorescence quenching for both trans and cis peptide bond conformations. Small peptides containing Pro-Tyr sequences, on the other hand, do not exhibit fluorescence quenching compared to Ac-Tyr-NHMe. Studies of fluorescence decay in the tryptic fragment of performic acid oxidized ribonuclease corresponding to residues 105–124 (i.e., O-T-16) demonstrate the presence of at least two environments of the single tyrosine chromophore (in the sequence Asn^{113}-Pro^{114}-Tyr^{115}). In these two (ensemble-averaged) environments, tyrosine has shorter and longer lifetimes, respectively, than in Ac-Tyr-NHMe. The fluorescence heterogeneity in O-T-16 does *not* correlate with X–Pro cis/trans conformational heterogeneity that can be detected by nuclear magnetic resonance (NMR) spectroscopy. Instead, the fluorescence heterogeneity in O-T-16 arises from the presence of multiple conformations with the same X–Pro peptide bond conformations which interconvert rapidly on the ^{1}H NMR time scale ($\tau \ll 1$ ms) but are distinguishable on the fluorescence lifetime time scale ($\tau \geq 1$ ns). From comparisons with the tyrosine fluorescence decay of smaller synthetic peptides, it is concluded that the long-lifetime tyrosine fluorescence component of O-T-16 arises from interactions involving residues outside the Asn^{113}-Pro^{114}-Tyr^{115}-Val^{116}-Pro^{117} sequence, which either stabilize particular local conformations in the vicinity of Tyr^{115} or act directly to protect Tyr^{115} from efficient fluorescence quenching. The short-lifetime component of O-T-16 is also observed for the pentapeptide Ac-Asn-Pro-Tyr-Val-Pro-NHMe. The data provide evidence for a nonrandom polypeptide conformation of O-T-16 under conditions of solvent pH and temperature at which the complete disulfide-intact ribonuclease molecule is fully folded. Implications of this work for the interpretation of fluorescence-detected unfolding experiments are discussed.

Over the last few years, many generalized mechanisms have been proposed to describe how native protein structures are regenerated from solvent-denatured (or, for disulfide-containing proteins, disulfide-reduced) predominantly disordered conformations (Kotelchuck & Scheraga, 1968; Scheraga, 1973; Ptitsyn, 1973; Wetlaufer, 1973; Tanaka & Scheraga, 1975, 1977; Karplus & Weaver, 1976; Schmid & Baldwin, 1978; Matheson & Scheraga, 1978; Némethy & Scheraga, 1979; Gō & Abe, 1981; Konishi et al., 1982; Lin & Brandts, 1983a; Mui et al., 1985). A common feature of many of these generalized mechanisms is a role for short-lived, local structures which form along the polypeptide chain in the initial stages of folding. For this reason, it is important to obtain experimental data on the structures in proteins which can arise from short- and medium-range interactions. For bovine pancreatic ribonuclease A, several experimental (Brown & Klee, 1971; Silverman et al., 1972; Bierzynski et al., 1982; Kim & Baldwin, 1982; Montelione et al., 1984; Lynn et al., 1984; Shoemaker et al., 1985) and theoretical (Pincus et al., 1983; Oka et al., 1984; Scheraga, 1985) studies of polypeptide fragments corresponding to proposed chain-folding initiation sites (Némethy & Scheraga, 1979) have been undertaken in order to identify conformations defined by local interactions under folding conditions. In addition, physical measurements have been made on disulfide-reduced, cysteine S-blocked ribonuclease (Schaffer, 1975; Takahashi et al., 1977, Chavez & Scheraga, 1980; Galat et al., 1981; Lord & Relyea, 1981; Swadesh et al., 1984) in order to identify local structures *under folding conditions*. These equilibrium studies have demonstrated that local interactions do indeed lead to ordered conformations that may form rapidly in the initial stages of folding, and they provide important structural information for the design of kinetic experiments which can identify intermediates on folding pathways.

Assuming a "growth-type" folding mechanism (Konishi et al., 1982), in which chain-folding initiation structures form with native (or nativelike) conformations, Némethy and Scheraga (1979) have proposed six amino acid sequences within ribonuclease A (designated as sites A–F) as likely sites

† This work was supported by research grants from the U.S./Israel Binational Science Foundation (217/84), the National Institute of General Medical Sciences of the National Institutes of Health (GM-24893), the National Science Foundation (DMB84-01811), and the NIH Resource for Multinuclear Magnetic Resonance at Syracuse University (RR-01317).

* Correspondence should be addressed to this author.

0006-2960/87/0426-1672$01.50/0

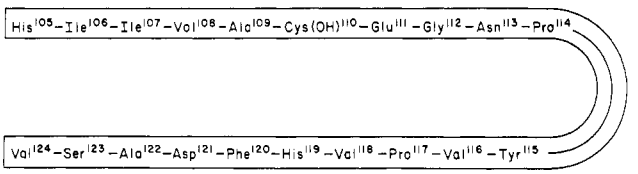

FIGURE 1: Amino acid sequence of a tryptic fragment of performic acid oxidized ribonuclease, O-T-16 (Hirs et al., 1956). The sequence numbers correspond to those of intact bovine pancreatic ribonuclease A. Cys(OH) refers to cysteic acid.

for chain-folding initiation. Significantly, part of one of these sequences (i.e., site F, which corresponds to residues 103–124) was also calculated to be the most (free) energetically favorable "hydrophobic nucleation site" (Matheson & Scheraga, 1978). Spectroscopic measurements (Montelione et al., 1984) on a synthetic fragment corresponding to residues 113–115 within chain-folding initiation site F, Ac-Asn-Pro-Tyr-NHMe,[1] revealed a strong tendency for this sequence to adopt a β-bend conformation (at Pro-Tyr) in water when the Asn–Pro peptide bond is trans; a type I β-bend (at Pro-Tyr) is also the conformation of Ac-Asn-Pro-Tyr-NHMe in the solid state (Montelione et al., 1984). Conformational energy calculations (Oka et al., 1984) indicated that there is a high bend probability (at Pro-Tyr) for Ac-Asn-Pro-Tyr-NHMe when the Asn–Pro peptide bond is trans and an even higher bend probability (at Asn-Pro) when the Asn–Pro peptide bond is cis (as it is in native ribonuclease). The implication of this work is that, in the initial stages of folding, a significant fraction of disulfide-reduced ribonuclease molecules should adopt β-bend structures within chain-folding initiation site F regardless of the peptide bond conformation at Asn^{113}-Pro^{114}.

As an extension of these equilibrium structural studies, we have undertaken spectroscopic studies of a tryptic fragment of performic acid oxidized ribonuclease A corresponding to residues 105–124 (Figure 1). This fragment, referred to as O-T-16[2] (Hirs et al., 1956), contains most of proposed chain-folding initiation site F and can be purified in large quantities by recently described procedures (McWherter et al., 1984). In addition, O-T-16 contains a single tyrosine residue (Figure 1), making it suitable for fluorescence lifetime studies that can identify very short-lived conformational states. Complementary tyrosine fluorescence lifetime and ^{1}H NMR spectroscopic data presented in this paper demonstrate the presence of locally ordered conformation(s) of O-T-16 in water at 25 °C which has (have) lifetime(s) that is (are) short relative to the ^{1}H NMR time scale (ca. 1 ms) but long relative to the tyrosine fluorescence decay time scale (ca. 1 ns).

Materials and Methods

Peptide Synthesis and Characterization. The syntheses of the terminally blocked amino acid Ac-Tyr-NHMe and the terminally blocked peptides Ac-Tyr-Pro-NHMe, Ac-Tyr-Pro-Asn-NHMe, Ac-Pro-Tyr-NHMe, Ac-Asn-Pro-Tyr-NHMe, and Ac-Asn-Pro-Tyr-Val-Pro-NHMe from L-amino acids, together with amino acid analyses, elemental analyses, and TLC data, have been described elsewhere (Stimson et al., 1982, 1986). These peptides were all >98% homogeneous when analyzed by reversed-phase HPLC on a Spectra Physics SP8000 liquid chromatography system using a gradient of 0–50% acetonitrile in 0.09% trifluoroacetic acid and 210-nm detection. The structures and homogeneity of these peptides, and of synthetic intermediates, were also verified by 300-MHz ^{1}H NMR spectroscopy. *p*-Cresol (4-methylphenol) was purified on reversed-phase HPLC by using the same column and conditions as for the peptides. The fluorescence homogeneity of these tyrosine-containing peptides was established by comparing their (uncorrected) fluorescence excitation (with excitation at 205–295 nm and detection at 301 nm) and fluorescence emission (with excitation at 277.5 nm and detection at 270–400 nm) spectra with those of Ac-Tyr-NHMe using a Perkin-Elmer Model MPF-44B fluorometer. All of these excitation and emission spectra have the same profile. No fluorescent contaminants were detected.

Preparation and Characterization of O-T-16. The tryptic fragment of performic acid oxidized ribonuclease corresponding to residues 105–124 was prepared by a peptide mapping procedure developed in our laboratory (McWherter et al., 1984); it was scaled up for the preparation of ribonuclease tryptic fragments in tens of milligram quantities. A 1-g sample of performic acid oxidized ribonuclease A was prepared according to the method of Hirs (1956). The tryptic digestion and separation of the resultant peptides were carried out as described previously (McWherter et al., 1984) except that a preparative-scale 2.5 × 21 cm reversed-phase Lichroprep RP-18 column (E. M. Merck) with a flow rate of 10 mL/min was used instead of the analytical-scale column.

The peak corresponding to O-T-16, whose elution position had previously been determined by analytical-scale chromatography, was collected and lyophilized. Amino acid analysis [Asx, 2.13 (2); Ser, 0.88 (1); Glx, 0.95 (1); Pro, 2.19 (2); Gly, 1.00 (1); Ala, 2.06 (2); Val, 3.89 (4); Leu, 0.02 (0); Ile, 1.46 (2); Tyr, 1.00 (1); Phe, 1.00 (1); His, 2.00 (2); Lys, 0.04 (0); Cys-SO_3, 0.94 (1)] confirmed the identity and purity of the sample, as did analytical-scale rechromatography. The fluorescence homogeneity of O-T-16 was also established by comparing its tyrosine fluorescence excitation and emission spectra with those of Ac-Tyr-NHMe, as described above; no fluorescent contaminants were observed. It has been shown elsewhere (Stimson et al., 1982) that, within the range of conditions used throughout this study, O-T-16 is monomeric.

Fluorescence Lifetime Measurements. For fluorescence measurements, samples were prepared either in distilled water, 0.1 M sodium acetate, redistilled dimethyl sulfoxide (Me_2SO) or in 6 M guanidine hydrochloride at peptide concentrations of ca. 10^{-4} M ($A_{276} \sim 0.20$). The pH of distilled water solutions was adjusted before each experiment either by addition of dilute (<0.02 M) buffer or by titration with dilute HCl or NaOH. Fluorescence decay kinetics were measured with an instrument based on the sampling oscilloscope technique (Hundley et al., 1967; Hazan et al., 1974; Hazan, 1973). A deuterium flash lamp (TRW, Inc.) with pulse duration of 5–6 ns was used as the excitation source. The excitation wavelength was selected by a Jarrel–Ash double monochromator (Model 82-410, 25 cm) (bandwidth 5 nm) or by a combination of an interference filter (Pomfret, Stamford) (transmission maximum 280 nm, bandwidth 12 nm) and a 1-cm path-length chemical filter composed of a mixture of $NiSO_4 \cdot 6H_2O$ (660

[1] Ac- and -NHMe designate terminal acetyl and *N*-methyl groups, respectively.

[2] Abbreviations: A_{276}, optical absorbance at 276 nm; Bicine, *N*,*N*-bis(2-hydroxyethyl)glycine; Cys(OH), cysteic acid; DCl, deuterium chloride; Me_2SO, dimethyl sulfoxide; DQF-COSY, two-dimensional double-quantum-filtered homonuclear-correlated proton magnetic resonance spectroscopy; D_2O, deuterium oxide; δ, chemical shift; Gdn·HCl, guanidine hydrochloride; HPLC, high-performance liquid chromatography; MOPS, 3-(*N*-morpholino)propanesulfonic acid; NMR, nuclear magnetic resonance; NOE, nuclear Overhauser effect; O-T-16, tryptic fragment of performic acid oxidized bovine pancreatic ribonuclease A corresponding to the 20 C-terminal amino acids; ppb, parts per billion; ppm, parts per million; rms, root mean square; TLC, thin-layer chromatography; DSS, 2,2-dimethyl-2-silapentane-5-sulfonate.

g/L) and 2,7-dimethyl-3,6-diazocyclohepta-1,6-diene perchlorate (2.5 g/L; 10:0.6 v/v) (Van Es & Wisse, 1963). The emission wavelength was selected by a combination of a Pyrex glass filter (with a cutoff at either 290 or 310 nm) and a Corning (Corning, NY) 3986 glass filter. These optical combinations result in high signal to noise ratios and very low stray light. The emitted light was detected with a Philips XP-1023 photomultiplier. In each experiment, the system response to pure solvent under identical conditions was also recorded and then subtracted from the fluorescence pulse (Haas et al., 1975).

The experimental decay curves were fitted to a calculated curve, $F_c(t)$

$$F_c(t) = \int_0^t G(t - s)I(s)\, ds \quad (1)$$

obtained by convolution of the instrument response to the lamp profile, $G(t)$, and the theoretical fluorescence decay function, $I(t)$:

$$I(t) = \sum_{i=1}^{n} \alpha_i \exp(-t/\tau_i) \quad (2)$$

where α_i and τ_i are the amplitude (preexponential factor) and lifetime, respectively, of the ith resolved fluorescent component. The parameters of eq 2 were optimized for both mono- (n = 1) and biexponential (n = 2) fits. The nonlinear least-squares fit algorithm NLIN (Marquardt, 1963) was used to calculate optimized parameters α_i and τ_i. The quality of the data fitting was evaluated by calculating the root mean square (rms) deviations between the experimental [$F(t)$] and calculated [$F_c(t)$] decay curves and by an evaluation of the randomness of the deviations between the experimental data and the best-fit theoretical curves. The randomness of these deviations was further analyzed by using the autocorrelation of residuals (Grinvald & Steinberg, 1974):

$$C(t_j) = \frac{1}{m}\sum_{i=1}^{m} R_i R_{i+j} \Big/ \frac{1}{n}\sum_{i=1}^{n} R_i^2 \quad (3)$$

where $R_i = F(t_i) - F_c(t_i)$ is the ith residual, n is the number of time intervals for which experimental data are available, and $m = n/2$.

The system was tested routinely for response linearity and time calibration by measuring the fluorescence decay of zone-refined anthracene (a kind gift of Dr. Z. Ludmer). For the fluorescence decay of an air-equilibrated solution of anthracene in cyclohexane, a lifetime of 4.05 ± 0.1 ns (Berlman, 1976) with an rms fit to a monoexponential decay of 0.0023 ± 0.0005 was routinely obtained. Peptides with tyrosine fluorophores gave even lower rms values when long averaging periods were employed. Experimental decay curves which did not show significantly improved rms deviations (reduction of the rms deviations by at least 0.0010) and lower autocorrelation of residuals when fit to an optimized biexponential decay are considered to be monoexponential fluorescence decay curves. All fluorescence measurements were made under atmospheric conditions.

^1H NMR Spectroscopy. ^{1}H NMR spectra were obtained on a Brüker WM-300 spectrometer at a proton resonance frequency of ca. 300 MHz. Samples were prepared either in >99.8% deuterium oxide (D_2O) containing 0.1 M deuterioacetic-d_4 acid adjusted to pH* [3] 3.00 ± 0.05 with deuterium chloride (DCl) or in dimethyl-d_6 sulfoxide (Me_2SO-d_6)/D_2O mixtures containing 10^{-3} M DCl. These deuteriated solvents

[3] pH* is the uncorrected pH meter reading of D_2O solutions.

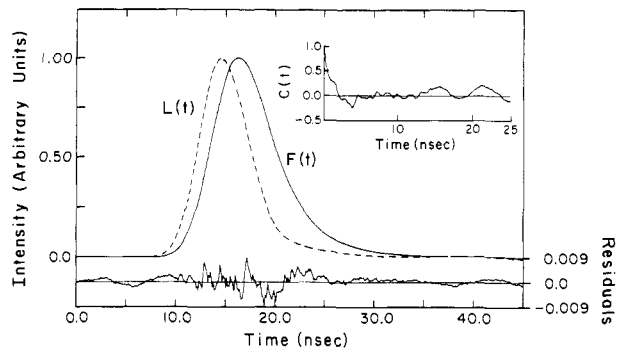

FIGURE 2: Fluorescence decay curve for Ac-Asn-Pro-Tyr-NHMe in distilled water (pH 7, 25 °C) fit to an optimized monoexponential decay with a lifetime τ of 2.2 ns. The rms deviation between the experimental curve and the theoretical monoexponential decay curve is 0.0021. The excitation pulse (276 nm, 5-nm bandwidth) is indicated by a dashed line [$L(t)$] and the resulting time-dependent fluorescence by a solid line [$F(t)$].

are products of Aldrich Chemical Co. The NMR measurements were made in 5-mm-diameter NMR tubes. Chemical shifts are reported relative to the methyl resonance of an internal standard of 2,2-dimethyl-2-silapentane-5-sulfonate (ca. 0.1 mM).

In quantitative measurements, the total spin recovery time between ca. 60° pulses (2.7 s) was sufficiently long to ensure complete relaxation of the peptide proton spin system. In measurements of the equilibria between minor and major peptide conformations, the spectra were resolution enhanced by transformation to a Gaussian free induction decay (Ferrige & Lindon, 1978) prior to Fourier transformation.

Double-quantum-filtered proton-correlated spectroscopy was carried out as described elsewhere (Piantini et al., 1982). Quadrature detection in the t_1 dimension was obtained by time-proportional phase incrementation (Redfield & Kunz, 1975; Marion & Wüthrich, 1983).

RESULTS

Fluorescence Lifetime Measurements. (A) Ac-Tyr-NHMe. The fluorescence decay of *N*-acetyl-L-tyrosine-*N'*-methylamide (Ac-Tyr-NHMe) was studied in H_2O, 0.1 M sodium acetate (pH 6.4), 6 M Gdn·HCl, and Me_2SO. These results are presented in Table I. Both in dilute aqueous buffers (≤0.02 M MOPS, pH 7.2) and in 6 M Gdn·HCl (pH 6.5), the tyrosine fluorophore exhibits a purely monoexponential decay, with a fluorescence lifetime of 2.2 ± 0.1 ns. The fluorescence lifetime of Ac-Tyr-NHMe was found to be 1.6 ± 0.1 ns (purely monoexponential) in 0.1 M sodium acetate. Quenching of phenol fluorescence by acetate is a well-known phenomenon (Kunimitsu et al., 1968). In Me_2SO solution, the fluorescence decay is also monoexponential with a reduced fluorescence lifetime of 1.6 ± 0.1 ns.

(B) X-Pro-Tyr Sequences. In order to examine the effect of X-Pro sequences on the fluorescence properties of tyrosine when it follows proline in the amino acid sequence, we studied the fluorescence decay of Ac-Pro-Tyr-NHMe, Ac-Asn-Pro-Tyr-NHMe, Ac-Ala-Pro-Tyr-NHMe, and Ac-Asn-Pro-Tyr-Val-Pro-NHMe. The X–Pro cis/trans peptide bond equilibrium constants, determined by ^{1}H NMR (Stimson et al., 1982, 1986) for these compounds in D_2O at 25 °C, are listed in Table I. Although both cis and trans X–Pro conformers of Ac-Pro-Tyr-NHMe, Ac-Asn-Pro-Tyr-NHMe, and Ac-Ala-Pro-Tyr-NHMe are populated under the conditions of the fluorescence lifetime measurements, these three compounds exhibit purely monoexponential fluorescence decay with a fluorescence lifetime (in unbuffered-aqueous solution at neutral

Table I: Tyrosine Fluorescence Measurements on Terminally Blocked[a] Tyr- and Pro-Containing Peptides

peptide[a]	solvent	τ_1[b] (ns)	τ_2[c] (ns)	α_1/α_2[d]	$K_{t\rightarrow c}$[e]	rms[f]
Tyr	H_2O[g]	2.2				0.0025 (m)
	6 M Gdn·HCl[h]	2.2				0.0021 (m)
	Me_2SO	1.6				0.0030 (m)
						0.0028 (b)
	0.1 M NaOAc	1.6				0.0027 (m)
Pro-Tyr	H_2O	2.2			0.33	0.0019 (m)
Asn-Pro-Tyr	H_2O	2.2			0.15	0.0021 (m)
Asn-Pro-Tyr-Val-Pro	H_2O	2.2	0.9	0.9 ± 0.2	0.15[i]	0.0027 (b)
						0.0062 (m)
	Me_2SO	1.4			<0.01	0.0029 (m)
	0.1 M NaOAc	1.6	0.6	0.5 ± 0.25		0.0025 (b)
						0.0035 (m)
Ala-Pro-Tyr	H_2O	2.1			0.28	0.0034 (m)
Tyr-Pro	H_2O, pH 7.5[j]	1.6	0.4	1.5 ± 0.2	0.55	0.0022 (b)
						0.0045 (m)
	Me_2SO	1.5				0.0045 (m)
Tyr-Pro-Asn	H_2O	1.5			0.33	0.0030 (m)
	6 M Gdn·HCl[h]	1.6				0.0026 (m)
	0.1 M NaOAc	1.2				0.0027 (m)

[a] *N*-Acetyl-*N'*-methyl amino acid and peptide amides. All measurements were made at room temperature. The excitation wavelength was 270 nm (when a monochromator was used to select the excitation wavelength) or 280 nm (when a filter was used to select the excitation wavelength). The emission was selected by a combination of a Pyrex glass with a cutoff at 300 nm and a Corning glass 3986 filter. [b] For monoexponential fluorescence decay, τ_1 is the fluorescence lifetime. For biexponential fluorescence decay, τ_1 is the fluorescence lifetime of the longer lived species. [c] For biexponential fluorescence decay, τ_2 is the fluorescence lifetime of the shorter lived species. [d] For biexponential fluorescence decay, α_1/α_2 is the ratio of the preexponential factors for the longer lived/shorter lived species. [e] For X–Pro compounds, $K_{t\rightarrow c}$ is the cis/trans equilibrium constant, as reported by Stimson et al. (1982, 1986). [f] Root-mean-square deviation between the observed fluorescence decay and either a monoexponential (m) or a biexponential (b) calculated decay curve. When the data were best fit to a monoexponential decay, the rms deviation for only the monoexponential fit is given. When the data were best fit to a biexponential decay, and when the data could be fit equally well to a mono- or biexponential decay, the rms deviations for both the mono- and biexponential fits are given for comparison. [g] Unless stated otherwise, measurements in H_2O were made at pH 6–7. [h] Measurements made in aqueous Gdn·HCl solutions were at an apparent pH of 6.5. [i] $K_{t\rightarrow c}$ is reported for the Asn–Pro peptide bond. No conformers with cis Val–Pro peptide bonds were observed. [j] A similar biexponential fluorescence decay was observed at pH 5.0.

pH) of 2.2 ± 0.1 ns (Table I and Figure 2). This value is similar to that observed for Ac-Tyr-NHMe, indicating little or no effect of *cis*- or *trans*-Pro on Tyr fluorescence in the X-Pro-Tyr sequence.

For Ac-Asn-Pro-Tyr-Val-Pro-NHMe in *dilute* (~0.005 M) sodium acetate solution at pH 6.5, the fluorescence decay is best fit to a biexponential decay (τ_1 = 2.2 ± 0.2 ns, τ_2 = 0.9 ± 0.2 ns, α_1/α_2 = 0.9 ± 0.2). The longer lived (τ_1 = 2.2 ns) fluorophore environment has a tyrosine fluorescence lifetime similar to those of Ac-Tyr-NHMe, Ac-Pro-Tyr-NHMe, Ac-Asn-Pro-Tyr-NHMe, and Ac-Ala-Pro-Tyr-NHMe (Table I). The shorter lived (τ_2 = 0.9 ns) tyrosine fluorophore environment of Ac-Asn-Pro-Tyr-Val-Pro-NHMe indicates that there are conformational or structural effects on the tyrosine fluorescence of the pentapeptide which are not present in the smaller Pro-Tyr-containing peptides. The significance of these results will be addressed under Discussion.

As was observed for Ac-Tyr-NHMe, higher sodium acetate buffer concentrations result in tyrosine fluorescence quenching. Both the short- and long-lived components of Ac-Asn-Pro-Tyr-Val-Pro-NHMe are quenched in 0.1 M sodium acetate, making it difficult to distinguish these two fluorescence components and resulting in only small deviations from apparent monoexponential fluorescence decay. In Me_2SO solution, the fluorescence decay of the pentapeptide is monoexponential with approximately the same lifetime (1.4 ns) as that of Ac-Tyr-NHMe in Me_2SO (1.6 ns).

(C) Tyr-Pro-Y Sequences. The conformational constraints of proline on residues preceding it in the amino acid sequence are well understood from theoretical studies (Schimmel & Flory, 1968; Zimmerman & Scheraga, 1977), including conformational free energy calculations (Oka et al., 1984) on Ac-Tyr-Pro-NHMe and Ac-Tyr-Pro-Asn-NHMe. The presence of proline in an amino acid sequence severely restricts the conformational space of the residue which precedes it [but not of the one which follows it (Zimmerman & Scheraga, 1977)] and can affect the distribution of tyrosine side-chain conformations in the Tyr-Pro-Y sequence. For this reason, it is interesting to compare the fluorescence properties of tyrosine when it precedes or follows proline.

Fluorescence decay data for Ac-Tyr-Pro-NHMe and Ac-Tyr-Pro-Asn-NHMe in H_2O at 25 °C are presented in Table I. In H_2O, both of these molecules exhibit average tyrosine fluorescence lifetimes significantly shorter than that of Ac-Tyr-NHMe. This quenching effect is attributable in part to the conformational effects of proline on the preceding tyrosine. Although Ac-Tyr-Pro-Asn-NHMe is best fit to a monoexponential decay with a fluorescence lifetime of 1.5 ± 0.1 ns, the tyrosine fluorescence decay of Ac-Tyr-Pro-NHMe is not monoexponential. Instead, the fluorescence decay of Ac-Tyr-Pro-NHMe is best described by a biexponential decay involving one component with a lifetime of 1.6 ± 0.10 ns and a second shorter lived component with a fluorescence lifetime of 0.4 ± 0.2 ns, having normalized preexponential terms of 0.6 ± 0.05 and 0.4 ± 0.05, respectively. Ac-Tyr-Pro-Asn-NHMe exhibits fluorescence quenching in 0.1 M sodium acetate, with a lifetime reduced by 26% ± 3% compared to its lifetime measured in much more dilute buffers (Table I). Quenching by phosphate ions was also observed (unpublished data). This reduction in fluorescence lifetime in 0.1 M sodium acetate is similar to that observed for other Tyr-containing peptides studied here. In Me_2SO solution, Ac-Tyr-Pro-NHMe has monoexponential decay with a lifetime (τ = 1.5 ns) similar to that measured for all the other Tyr-containing peptides in Me_2SO.

In order to investigate the quenching of tyrosine in these Tyr-Pro-Y peptides further, we measured the relative quantum yields, Q_f', of Ac-Tyr-Pro-NHMe and Ac-Tyr-Pro-Asn-NHMe (relative to that of Ac-Tyr-NHMe) by steady-state fluorescence measurements at room temperature (Table II).

Table II: Integrated Fluorescence Data

peptide[a]	Q_f'[b]	Q_τ[c]	Q_f'/Q_τ
Tyr	2.20	2.2 ± 0.1	1.00
Tyr-Pro	1.05 ± 0.05	1.1 ± 0.1	0.95 ± 0.1
Tyr-Pro-Asn	1.15 ± 0.05	1.5 ± 0.1	0.75 ± 0.1

[a] *N*-Acetyl-*N'*-methyl amino acid and peptide amides. All measurements were made at room temperature in H_2O. [b] Relative quantum yield, arbitrarily normalized to the fluorescence lifetime of Tyr (viz., 2.20 ns) in Ac-Tyr-NHMe. $Q_f' = 2.20\ (F_{peptide}/A_{276,peptide})/(F_{Ac\text{-}Tyr\text{-}NHMe}/A_{276,Ac\text{-}Tyr\text{-}NHMe})$ where F is the integrated fluorescence emission profile. [c] $Q_\tau = \sum_i \alpha_i\tau_i/\sum_i \alpha_i$ is the quantum yield calculated from the time-resolved fluorescence decay parameters.

Table III: Tyrosine Fluorescence Lifetime Measurements on O-T-16[a]

solvent	τ_1[b] (ns)	τ_2[c] (ns)	α_1/α_2[d]	rms[e]
H_2O, pH 6	3.6 ± 0.5	1.5 ± 0.2	0.18 ± 0.05	0.0030 (b)
	2.0 ± 0.2			0.0060 (m)
0.1 M sodium	2.5 ± 0.5	1.2 ± 0.1	0.18 ± 0.08	0.0025 (b)
acetate, pH 6.4	1.5 ± 0.1			0.0050 (m)
0.02 M Bicine,	3.4 ± 0.5	1.5 ± 0.1	0.14 ± 0.05	0.0025 (b)
pH 7.5	1.7 ± 0.1			0.0050 (m)
H_2O, pH 8.3	4.2 ± 0.6	1.4 ± 0.15	0.19 ± 0.04	0.0065 (b)
(λ_{em} >335	2.2 ± 0.2			0.0164 (m)
nm)[f]	3.6 ± 0.5	1.3 ± 0.15	0.22 ± 0.04	0.0025 (b)
	2.0 ± 0.2			0.0123 (m)
6 M Gdn·HCl[g]	3.7 ± 0.5	1.5 ± 0.15	0.17 ± 0.05	0.0028 (b)
	2.1 ± 0.2			0.0082 (m)
Me_2SO	1.5 ± 0.15			0.0025 (m)
	1.5 ± 0.15			0.0023 (b)

[a] Measurements were carried out at room temperature. The excitation wavelength was either 270 nm (when the excitation wavelength was selected by a monochromator) or 280 nm (when the excitation wavelength was selected by a filter). The emission was selected by a combination of a Pyrex glass with a cutoff at 290 or 310 nm and a Corning 3986 filter. [b] For monoexponential fluorescence decay, τ_1 is the fluorescence lifetime. For biexponential fluorescence decay, τ_1 is the fluorescence lifetime of the longer lived species. [c] For biexponential fluorescence decay, τ_2 is the fluorescence lifetime of the shorter lived species. [d] For biexponential fluorescence decay, α_1/α_2 is the ratio of the preexponential factors for the longer lived/shorter lived species. [e] Root-mean-square deviation between the observed fluorescence decay and either a monoexponential (m) or a biexponential (b) calculated decay curve. When the data were best fit to a biexponential decay, or when the data could be fit equally well to a mono- or biexponential decay, the rms deviations for both the mono- and biexponential fits are given for comparison. [f] Fluorescence emission was detected at 335–380 nm, using Schott WG 335 and Corning Glass 3986 filters. The high rms deviation is due to the low light level at the red edge of tyrosine emission. [g] Measurement made in aqueous Gdn·HCl solutions at an apparent pH of 6.5.

For both of these peptides, the tyrosine quantum yields are significantly lower than that of Ac-Tyr-NHMe. Hence, interresidue interactions within these peptides result in tyrosine fluorescence quenching. The ratios of these steady-state quantum yields to the corresponding quantum yields calculated from time-resolved fluorescence measurements are presented in Table II. This ratio (Q_f'/Q_τ where $Q_\tau = \sum_i \alpha_i\tau_i/\sum_i \alpha_i$) is a measure of the fraction of molecules whose fluorescence contributes to the steady-state fluorescence emission. If this ratio is less than unity, it indicates that, in a fraction of the fluorophores, the fluorescence lifetime is reduced to a range which is too fast to be measured in these time-resolved experiments. For Ac-Tyr-Pro-NHMe, the ratio Q_f'/Q_τ is approximately unity (Table II), and the tyrosine quenching is completely accounted for by its two quenched components. For Ac-Tyr-Pro-Asn-NHMe, on the other hand, the ratio Q_f'/Q_τ is 0.75 ± 0.1, indicating that approximately 25% of the fluorophores exhibit static quenching; that is, their fluorescence lifetime is too short to measure by our time-resolved experiments. The remaining ~75% of molecules are characterized by the single long lifetime, resulting in an apparent monoexponential decay. The static quenching in Ac-Tyr-Pro-Asn-NHMe indicates the existence of a population of conformers with specific intramolecular interactions affecting the phenol ring, with a conformational lifetime longer than that of the excited state of tyrosine. This conclusion is consistent with results of conformational energy calculations on Ac-Tyr-Pro-Asn-NHMe (Oka et al., 1984) which indicate that, for the predominant conformational ensemble with trans Tyr–Pro bonds, extended backbone conformations with Tyr $O^\eta H\cdots O^\delta$ Asn side-chain/side-chain hydrogen bonds have the lowest conformational free energy.

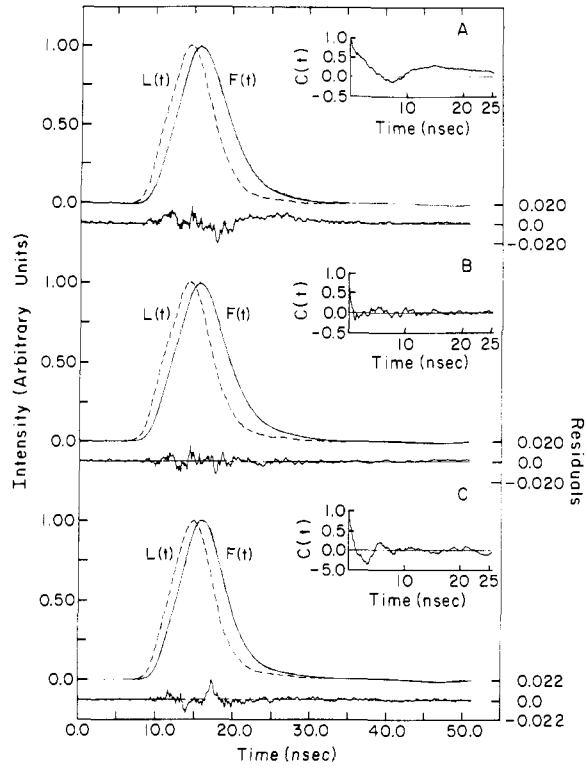

FIGURE 3: Fluorescence decay curves for O-T-16. (A) O-T-16 in 0.02 M Bicine buffer (pH 7.5, 25 °C) fit to an optimized monoexponential decay with a lifetime of 1.7 ns. The rms deviation between the experimental and theoretical decay curves is 0.005. (B) The same experimental curve as in (A) reanalyzed and fit to a biexponential decay, with component lifetimes of 3.4 ns (α_1 = 0.12) and 1.5 ns (α_2 = 0.88). The rms deviation between the experimental and theoretical decay curves is 0.0025. (C) O-T-16 in Me_2SO (25 °C) fit to an optimized monoexponential decay with a lifetime of 1.5 ns. The rms deviation between experimental and theoretical decay curves is 0.0025. $L(t)$, excitation pulse profile; $F(t)$, fluorescence response.

(*D*) *Residues 105–124 of Performic Acid Oxidized Ribonuclease* (*O-T-16*). In order to examine the hypothesis that short- and medium-range interactions can define local conformations within proposed chain-folding initiation site F (i.e., residues 103–124), we also examined the fluorescence decay kinetics of O-T-16, a tryptic fragment corresponding to residues 105–124 of performic acid oxidized ribonuclease A. This 20 amino acid long fragment (Figure 1) contains a single tyrosine residue and two prolines (in the sequence Asn^{113}-Pro^{114}-Tyr^{115}-Val^{116}-Pro^{117}-Val^{118}).

Fluorescence lifetime data and decay kinetics for O-T-16 in water are presented in Table III and in Figure 3, respectively. As can be seen by comparing Figure 3A and Figure 3B, in H_2O at 25 °C the fluorescence decay of O-T-16 is not monoexponential (the poor correlation function presented in the inset of Figure 3A for the optimal monoexponential fit

should be noted). In several measurements in H_2O, over the pH range 6–8, the fluorescence of O-T-16 is optimally fit to a biexponential decay (Figure 3B) with lifetimes $\tau_1 \approx 3.6$ ns and $\tau_2 \approx 1.5$ ns (Table III). In aqueous solutions at 25 °C, the ratio of the long-lifetime (3.6 ns) to the short-lifetime (1.5 ns) preexponential factors is 0.18 ± 0.05.

The heterogeneous fluorescence decay of O-T-16 cannot be attributed to intermolecular aggregation effects, since the molecule is monomeric at the dilute concentrations used for these fluorescence measurements (see Materials and Methods). The purity of the preparation was double checked by a second preparative fractionation on a different reverse-phase column without any effect on the decay parameters. Also, the (uncorrected) tyrosine fluorescence excitation and emission profiles of O-T-16 were observed to be identical with those of Ac-Tyr-NHMe (and of the other Tyr-containing peptides), indicating no fluorescent contaminants. In addition, the heterogeneous decay cannot be attributed to multiple, noninterconvertible electronic excited states, as has been proposed for certain Trp-containing peptides (Rayner & Szabo, 1978), since both Ac-Tyr-NHMe and Ac-Asn-Pro-Tyr-NHMe, which should have Tyr electronic excited states similar to those of O-T-16, exhibit monoexponential fluorescence decay. These considerations lead to the conclusion that the multiexponential decay of O-T-16 can be attributed to multiple ground-state molecular conformations which interconvert at a rate slower than (or equal to) the rate of fluorescence decay.

To provide supporting evidence for this interpretation, we attempted to alter the equilibrium between the conformations which are distinguished in the time-resolved fluorescence measurements by altering the solvent. In 6 M Gdn·HCl, the tyrosine fluorescence decay is biexponential with decay parameters similar to those observed in water (Table III). This result indicates that the interactions responsible for the heterogeneous fluorescence of O-T-16 are not disrupted in 6 M Gdn·HCl. On the other hand, in Me_2SO the tyrosine fluorescence exhibits monoexponential decay (Table III and Figure 3C) with a lifetime (1.5 ± 0.1 ns) similar to that of the shorter lived conformer(s) which is (are) present in water. This change from multi- to monoexponential fluorescence decay could arise either from a direct quenching effect of Me_2SO solvent on the tyrosine fluorophore or from an indirect effect of Me_2SO on the conformational distribution of fluorophore environments. In order to distinguish direct and conformational effects of Me_2SO on O-T-16 tyrosine fluorescence, we also examined the time-resolved fluorescence decay of *p*-cresol (4-methylphenol), a model compound which consists of the phenol fluorophore of the side chain of tyrosine without the peptide backbone.

In 0.05 M Bicine buffer (pH 7.5, 25 °C), the fluorescence decay of *p*-cresol is monoexponential with a fluorescence lifetime of 2.9 ± 0.15 ns. This lifetime is significantly longer than those of the other Tyr-containing peptides listed in Table I, indicating that backbone/side-chain interactions in these peptides result in intramolecular tyrosine fluorescence quenching. The effect of titration with Me_2SO on the time-resolved fluorescence of *p*-cresol is shown in Figure 4. A monoexponential fluorescence decay was observed throughout the solvent titration curve. Between 0 and ca. 50% Me_2SO, the fluorescence lifetime of *p*-cresol appears to be solvent independent (τ = 2.9 ± 0.1 ns), while above 50% Me_2SO a decreased lifetime, attributable to significant fluorescence quenching by the solvent, is observed. These data indicate that there is little or no direct effect of Me_2SO titration on tyrosine fluorescence in <50% Me_2SO/aqueous Bicine buffer solutions.

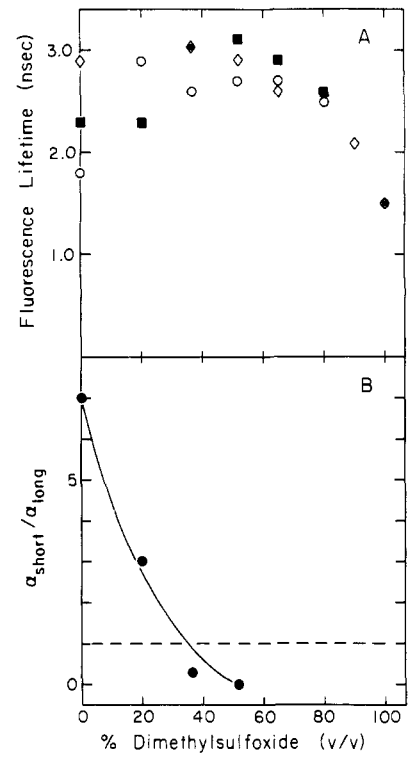

FIGURE 4: Time-resolved tyrosine fluorescence parameters in 0.05 M Bicine (pH 7.5)/Me_2SO mixed systems. (A) Fluorescence lifetimes for *p*-cresol (◊), Ac-Tyr-NHMe (■), and O-T-16 (○). For O-T-16, the value for the weighted average lifetime is plotted, since the decay is not monoexponential in <50% Me_2SO. (B) Ratio of short- to long-lifetime preexponential factors for O-T-16 in mixed solvent systems. The dashed line is drawn for $\alpha_{short}/\alpha_{long} = 1$.

The solvent titration of the time-resolved fluorescence of Ac-Tyr-NHMe with Me_2SO is also shown in Figure 4. In all of these mixed solvent systems, the fluorescence decay of Ac-Tyr-NHMe was monoexponential. Between 0 and ca. 50% Me_2SO, the fluorescence lifetime increases from 2.3 ± 0.1 to 3.1 ± 0.1 ns. These data indicate conformation-dependent quenching in aqueous Ac-Tyr-NHMe which is relieved by altering the distribution of molecular conformations. Above ca. 50% Me_2SO, the fluorescence data cannot be interpreted in terms of conformational effects since there is additional direct quenching by Me_2SO like that observed for *p*-cresol.

We next examined the effect of Me_2SO titration on the time-resolved fluorescence of O-T-16. These data are also shown in Figure 4. In 20% Me_2SO, the fluorescence decay kinetics are fit to biexponential decays with lifetimes (τ_1 = 3.4 ± 0.2 ns, τ_2 = 1.7 ± 0.2 ns) similar to those measured in the absence of Me_2SO (Table III). However, in 20% Me_2SO, the relative contribution of the long-lifetime component is nearly twice that measured in the absence of Me_2SO (Figure 4B), indicating a solvent-dependent shift in the equilibrium between long- and short-lived conformational ensembles. With increasing Me_2SO concentration, the long-lifetime component becomes dominant, and in 50% Me_2SO, the shorter lifetime component is not even detected (Figure 4B). Above ca. 50% Me_2SO, direct solvent quenching (like that observed in *p*-cresol) becomes important, and conclusions about conformational distributions cannot be drawn from the fluorescence data.

The Me_2SO titration of the solvent-dependent equilibrium in O-T-16 could be followed by measurements of either the average time-resolved fluorescence lifetimes (Figure 4A) or the ratio of preexponential factors (Figure 4B). This same solvent-dependent equilibrium could be followed with

steady-state fluorescence measurements (although a slight shift of the fluorescence emission of both Ac-Tyr-NHMe and O-T-16 toward longer wavelengths with increasing Me_2SO was observed). For both Ac-Tyr-NHMe and O-T-16, the dependence of the quantum yield on Me_2SO concentration is very similar to that of the dependence of the average fluorescence lifetime determined by time-resolved measurements (data not shown). Both peptides exhibit longer lifetimes (and higher quantum yields) in 20–50% Me_2SO than in the absence of Me_2SO. For O-T-16, this effect is significantly larger than for Ac-Tyr-NHMe. These results indicate that both Ac-Tyr-NHMe and O-T-16 exhibit conformation-dependent fluorescence quenching in aqueous solution which is relieved by Me_2SO titration (up to ca. 50% Me_2SO). The conformation-dependent quenching in O-T-16 may arise both from local backbone/side-chain interactions (similar to those present in Ac-Tyr-NHMe) and from longer range conformational effects which are perturbed by Me_2SO. Clearly, conformations with longer lifetimes are stabilized relative to the conformations with shorter lifetimes, with increasing Me_2SO concentration (up to ca. 50% Me_2SO).

^1H NMR Spectroscopy. In the preceding section, we presented evidence (based on fluorescence lifetime measurements) for multiple conformations of O-T-16 in the vicinity of Tyr^{115} in water under conditions of solvent and temperature at which the complete disulfide-intact ribonuclease molecule is folded. In related work (Stimson et al., 1982), we have observed that, in ^1H NMR spectra of O-T-16 (in water), the Tyr^{115} ring resonances are also sensitive to a conformational equilibrium, tentatively attributed to cis/trans Asn^{113}–Pro^{114} peptide-bond isomerization. In water, the fraction of the minor conformation which is detected in the ^1H NMR spectra (12% ± 1% at 25 °C) is similar to the percentage of O-T-16 molecules with a long fluorescence lifetime (18% ± 5% in water at 25 °C). However, these two spectroscopic techniques probe different dynamic time scales and may therefore be sensitive to different conformational equilibria. In order to determine if the minor conformer(s) detected by fluorescence is (are) identical with those detected by NMR, we compared the effects of solvent perturbation on the conformational equilibria detected by the NMR and fluorescence lifetime spectroscopies.

(A) Major Aromatic Proton Resonances. The aromatic region of the ^1H NMR spectrum of O-T-16 (at pH* 3.0, 25 °C) is presented in Figure 5. In this resolution-enhanced (Ferrige & Lindon, 1978) spectrum, both major and minor aromatic resonances of O-T-16 are observed. The significance and identification of these minor resonances are discussed below.

The resonances of the single tyrosine of O-T-16 have been assigned previously (Stimson et al., 1982). Besides these tyrosine aromatic resonances of the major O-T-16 conformer, minor tyrosine aromatic resonances (at 7.09, 6.84, and 6.78 ppm) are also observed. The significance of these minor resonances, which correspond to conformations of O-T-16 in slow-exchange equilibrium with the predominant conformation(s), is discussed in detail below.

At pH* 3.0, two major His $C^\epsilon H$ resonances are observed (Figure 5) at 8.69 and 8.60 ppm, respectively, which correspond to the two histidines (His^{105} and His^{119}) in O-T-16. These two major His $C^\epsilon H$ resonances were tentatively assigned by comparing the His $C^\epsilon H$ chemical shifts with those of disulfide-reduced, S-sulfonated ribonuclease, for which all four $C^\epsilon H$ resonances have been assigned (Swadesh et al., 1984) by selective partial deuteriation (Markley, 1975). In this disulfide-reduced derivative of ribonuclease A, the His^{105} $C^\epsilon H$ and His^{119} $C^\epsilon H$ protons have resonance frequencies of 8.59 and 8.60 ppm, respectively, in 0.1 M deuterioacetic acid at pH* 3.0 and 25 °C (Swadesh et al., 1984). Indeed, under these conditions, all four His $C^\epsilon H$ resonances of S-sulfonated ribonuclease have chemical shifts in the range of 8.60 ± 0.01 ppm. Comparing these chemical shifts with the His $C^\epsilon H$ chemical shifts of O-T-16, it is clear that one of the O-T-16 histidine resonances (at 8.69 ppm) has a significantly perturbed chemical shift (ca. 0.1 ppm). Since His^{105} is the N-terminal residue of O-T-16, its chemical shift will be perturbed by its positively charged amino group (at pH* 3.0). On this basis, the resonances of O-T-16 at 8.69 (perturbed) and 8.60 ppm are assigned to the His^{105} and His^{119} $C^\epsilon H$ protons, respectively.

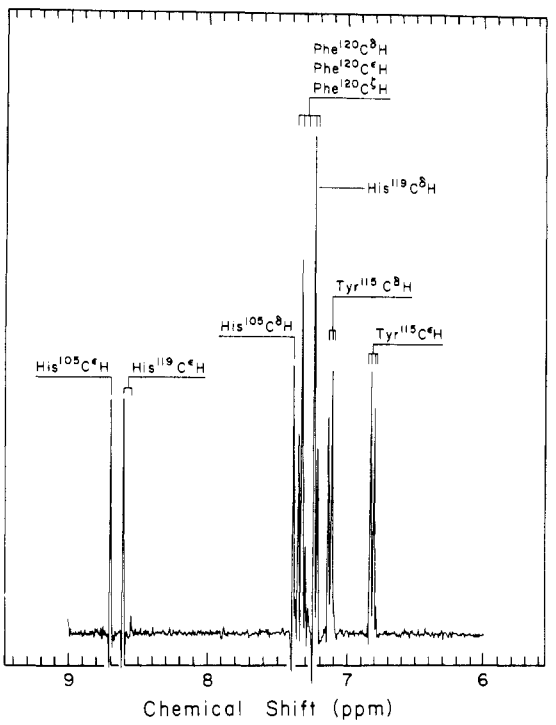

FIGURE 5: Aromatic resonances of 300-MHz ^1H NMR spectrum of 0.7 mM O-T-16 in 0.1 M deuterioacetic-d_4 acid, pH* 3.0, 25 °C.

At pH* 3.0 and 25 °C, the His $C^\delta H$ and Phe ring proton resonances of O-T-16 are overlapped (Figure 5). The major His $C^\delta H$ resonances of O-T-16 were identified from His $C^\delta H/C^\epsilon H$ cross-peaks in DQF-COSY (data not shown). From this correlated spectrum, the resonances at 7.38 and 7.23 ppm are assigned to the His^{105} and His^{119} $C^\delta H$ protons, respectively. The remaining O-T-16 aromatic ring resonances (7.35, 7.32, 7.30, 7.23, and 7.21 ppm at pH* 3.0, 25 °C) are assigned to the Phe^{120} aromatic ring proton resonances (Figure 5) on the basis of the system of spin–spin couplings observed in the DQF-COSY spectrum.

(B) Minor Resonances of O-T-16. An expanded region of the spectrum shown in Figure 5 is presented in Figure 6A. Minor Tyr $C^\epsilon H$ resonances (at 6.78 and 6.84 ppm) and a minor Tyr $C^\delta H$ resonance (at 7.09 ppm) indicate the presence of multiple O-T-16 conformations which interconvert slowly relative to the 300-MHz ^1H NMR chemical shift time scale (viz., with lifetimes $\gg$ 1 ms). The two minor Tyr $C^\epsilon H$ resonances differ in frequency by 27 Hz (independent of the sample spinning rate), which is too large to be attributed to three-bond coupling between the ϵ- and δ-tyrosine protons of a single minor conformer. Instead, this large frequency difference is attributed to two distinct minor O-T-16 conformations [designated *xy* conformer(s) and *yx* conformer(s)] which are in equilibrium with the major conformation(s)

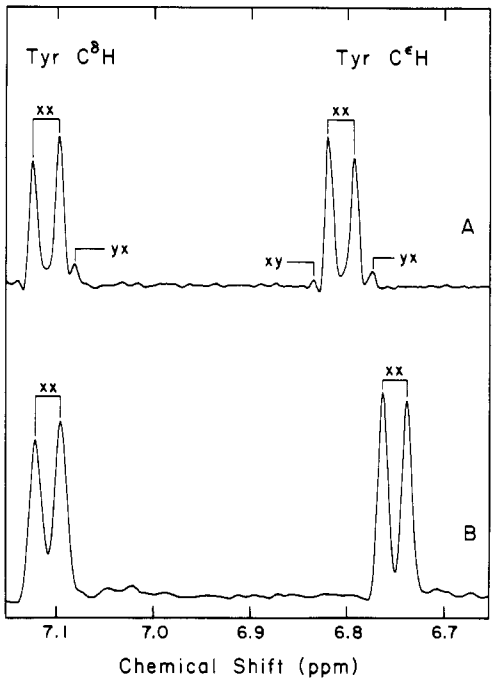

FIGURE 6: (A) Expansion of tyrosine resonances of 0.7 mM O-T-16 in D_2O at pH* 3.0, 25 °C. The notation, *xx*, *xy*, and *yx* is discussed in the text. (B) Expansion of tyrosine resonances of O-T-16 in 50% (v/v) Me_2SO-d_6 in D_2O (10^{-3} M DCl) at 25 °C.

(designated *xx*). The use of two letters to characterize each of these conformational ensembles indicates that the conformational differences exist at two different sites. Portions of the minor Tyr C$^{\epsilon}$H doublet resonances are overlapped with the Tyr C$^{\epsilon}$H doublet of the major conformation(s). Similarly, the small upfield (partially overlapped) Tyr^{115} C$^{\delta}$H doublet is assigned to the minor *yx* conformation(s), since it has about the same relative intensity as the Tyr C$^{\epsilon}$H *yx* conformation(s). These conclusions were verified by an analysis of the fine structure of the Tyr C$^{\delta}$H/C$^{\epsilon}$H cross-peaks of the absorption-mode DQF-COSY spectrum obtained in D_2O at pH* 3.5, 27 °C. The Tyr C$^{\delta}$H/C$^{\epsilon}$H cross-peak fine structure indicates three distinct two-spin systems, arising from the *xx* (major), *xy*, and *yx* conformational ensembles (data not shown). Furthermore, the ratios of *yx*:*xx* and *xy*:*xx* peak intensities are different, indicating that the resonances labeled *xy* and *yx* do not arise from restricted Tyr ring rotation of a single minor conformer.

A minor His C$^{\epsilon}$H resonance (8.55 ppm) of O-T-16 is also observed in D_2O (Figure 5). This resonance was identified as a minor resonance of His^{119} C$^{\epsilon}$H by comparing the normalized integrated area of the His^{105} (1.00), major His^{119} (0.90), and minor His^{119} (0.10) C$^{\epsilon}$H resonances, in the absence of resolution enhancement. Cross-peaks between the *minor* His^{119} C$^{\epsilon}$H and C$^{\delta}$H protons were not observed in the DQF-COSY spectrum since these cross-peaks arise from four-bond coupling and are much weaker than the minor Tyr C$^{\delta}$H/C$^{\epsilon}$H cross-peaks discussed above. For this reason, the minor His^{119} C$^{\delta}$H resonance could not be identified. From data described below, the minor His^{119} C$^{\epsilon}$H resonance appears to be associated with the minor *yx* conformational ensemble.

The relative populations of *xx*, *xy*, and *yx* conformations are in solvent-dependent equilibrium, since no minor resonances of the Tyr ring (or His C$^{\epsilon}$H resonances) are observed in solutions containing more than 50% Me_2SO-d_6 (Figure 6B). In order to compare the solvent dependence of the conformational equilibria detected by ^{1}H NMR and by fluorescence lifetime measurements, respectively, we also obtained ^{1}H

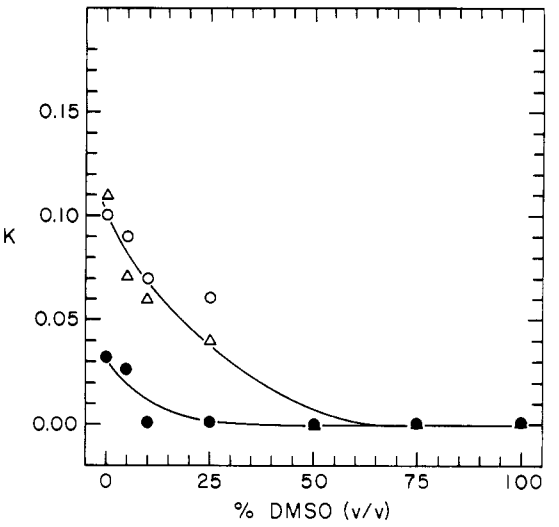

FIGURE 7: Dependence of conformational equilibria detected by NMR on Me_2SO-d_6 concentration. (△) Ratio of minor to major His^{119} C$^{\epsilon}$H resonance intensities; (○) ratio of minor *yx* to major *xx* Tyr^{115} resonance intensities (averaged between Tyr C$^{\delta}$H and Tyr C$^{\epsilon}$H); (●) ratio of minor *xy* to major *xx* Tyr^{115} C$^{\epsilon}$H resonance. The solvents were mixtures of Me_2SO-d_6 and D_2O containing 10^{-3} M DCl.

NMR spectra at several Me_2SO:D_2O solvent ratios. The relative chemical shifts of the minor and major resonances were unaffected by the Me_2SO titration (although these chemical shifts, relative to DSS, do depend on the concentration of Me_2SO). The solvent-dependent *xy*:*xx* and *yx*:*xx* tyrosine resonance intensity ratios are plotted in Figure 7. No *xy* or *yx* conformers were detected in aqueous solutions containing more than 25% or 50%, respectively, Me_2SO-d_6.

The ratio of the minor to major His^{119} C$^{\epsilon}$H conformers is also solvent dependent, and the dependence of this ratio on Me_2SO-d_6 concentration is also plotted in Figure 7. This ratio of minor to major His^{119} C$^{\epsilon}$H resonances is identical with that of the *yx*:*xx* ratio detected by the tyrosine resonances over the entire range of Me_2SO-d_6 concentrations (Figure 7), indicating that the His^{119} C$^{\epsilon}$H resonances and both the Tyr^{115} C$^{\epsilon}$H and Tyr^{115} C$^{\delta}$H resonances reflect the same conformational equilibrium, viz., the *yx*/*xx* equilibrium. This indicates that there is a strong correlation between the conformational states of the His^{119} and Tyr^{115} side chains in water and in <50% Me_2SO-d_6/D_2O solvent mixtures.

Comparing Figure 4B and Figure 7, it is clear that the conformational equilibria detected by the Tyr and His aromatic ring resonances of O-T-16 do not correspond to the conformational equilibrium which is distinguished by long and short tyrosine fluorescence lifetimes. Between 0% and 50% Me_2SO, the major *xx* conformational ensemble is selectively stabilized, while over this same solvent titration range there is a shift from predominantly short-lifetime fluorophores to predominantly long-lifetime fluorophores. Indeed, in ca. 30% Me_2SO, approximately equal amounts of long and short fluorescence-lifetime conformers are present in equilibrium, while >95% *xx* ensemble is measured by ^{1}H NMR. Hence, the two (or more) conformers distinguished by the tyrosine fluorescence lifetime measurements arise primarily from subpopulations of the *xx* conformational ensemble. While these two conformers interconvert slowly (within the *xx* conformational ensemble) relative to the fluorescence lifetime time scale, they interconvert rapidly relative to the proton chemical shift time scale.

Discussion

Fluorescence Quenching in Tyr-Pro-Y Peptides. Steady-

state fluorescence measurements indicate that the fluorescence of tyrosine in Ac-Tyr-Pro-NHMe and Ac-Tyr-Pro-Asn-NHMe is quenched relative to that of Ac-Tyr-NHMe. The quenching is due to intramolecular interactions involving the phenol fluorophore. In order to gain a better understanding of the conformational features that give rise to this fluorescence quenching, we have compared these results of fluorescence spectroscopy with the results of NMR measurements on these same peptides.

The fluorescence decay measurements on Ac-Tyr-Pro-NHMe indicate that there are at least two conformational ensembles with different (ensemble-averaged) fluorescence lifetimes (i.e., $\tau_1 = 1.6 \pm 0.15$ ns and $\tau_2 = 0.4 \pm 0.15$ ns). Interconversion between these ensembles is slower than (or equal to) the nanosecond excited-state lifetimes. Within each ensemble, the (ensemble-averaged) fluorescence lifetime is shorter than that of Ac-Tyr-NHMe ($\tau = 2.2$ ns). These quenched lifetimes result from dynamic quenching. That is to say, the lifetimes of the interactions responsible for the fluorescence quenching (within each ensemble) are comparable to or shorter than the corresponding excited-state lifetimes.

From ^{1}H and ^{13}C NMR measurements (Stimson et al., 1982), we have established that Ac-Tyr-Pro-NHMe exists as an equilibrium mixture of cis and trans Tyr–Pro peptide bond conformers in water at 25 °C. The cis/trans equilibrium constant determined by NMR, $K_{t\rightarrow c} = 0.55 \pm 0.05$, is similar to the ratio of minor ($\tau_2 = 0.4 \pm 0.2$ ns, $\alpha_2 = 0.4 \pm 0.04$) to major ($\tau_1 = 1.6 \pm 0.1$ ns, $\alpha_1 = 0.6 \pm 0.04$) fluorescence decay preexponential factors, $\alpha_2/\alpha_1 = 0.7 \pm 0.1$, suggesting that the minor ($\tau_2 = 0.4$ ns) conformational ensemble of Ac-Tyr-Pro-NHMe detected by time-resolved fluorescence measurements may correspond to the set of molecular conformations with cis Tyr–Pro peptide bonds. This correlation, however, is not unique, and from the experiments described here, we cannot rule out the possibility that the interconversion between short- and long-lifetime conformers involves some other conformational isomerization. *In either interpretation*, however, *cis/trans*-proline isomerization in Ac-Tyr-Pro-NHMe will result in a change in the average fluorescence emission since the *cis/trans*-proline equilibrium is coupled to other conformational equilibria within the trans (and cis) ensembles. Hence, an alteration of the *cis/trans*-proline equilibrium of Ac-Tyr-Pro-NHMe will be accompanied by a change in the steady-state fluorescence properties of the peptide. This change in fluorescence would arise purely from a change in *short-range* quenching interactions within the Ac-Tyr-Pro-NHMe sequence in any polypeptide in which this sequence occurs.

For Ac-Tyr-Pro-Asn-NHMe, the fluorescence decay is monoexponential, with a lifetime $\tau_1 = 1.5 \pm 0.1$ ns. Comparison of the relative fluorescence quantum yield calculated from steady-state measurements (Q_f') to the fluorescence quantum yield calculated from the fluorescence decay (Q_τ) reveals a second population of molecules that do not contribute to the integrated time-resolved fluorescence, i.e., fluorescent molecules with very short fluorescence lifetimes. This fraction, 25% ± 10%, is similar to the fraction of molecules with cis Tyr–Pro peptide bonds, identified by ^{13}C and ^{1}H NMR spectroscopy (Stimson et al., 1982), 29% ± 2%. As for Ac-Tyr-Pro-NHMe, however, we cannot exclude the possibility that the interconversion between the two conformational ensembles corresponds to an isomerization process other than peptide bond isomerization. In either case, the results demonstrate that cis/trans isomerization in Ac-Tyr-Pro-Asn-NHMe will be accompanied by a change in the average fluorescence emission which results from a change in the distribution of local quenching interactions.

In 6 M Gdn·HCl, the tyrosine fluorophore of Ac-Tyr-Pro-Asn-NHMe is also quenched relative to Ac-Tyr-NHMe and exhibits a monoexponential fluorescence decay ($\tau_1 = 1.6 \pm 0.15$ ns). This result indicates that, in the guanidine-induced denaturation of ribonuclease A, fluorescence changes due to *local quenching effects* will accompany any *cis/trans*-proline isomerization that takes place subsequent to rapid overall unfolding of the protein.

Assignment of xx, xy, and yx Conformers of O-T-16 Observed in ^{1}H NMR Spectra. From the ^{1}H NMR spectra of the aromatic resonances of O-T-16, we have identified three distinct conformational ensembles (viz., *xx*, *xy*, and *yx* ensembles) of O-T-16 which are in slow exchange on the ^{1}H NMR time scale, i.e., with lifetimes $\gg 1$ ms. A possible interpretation for this chemical shift heterogeneity is the presence of an equilibrium mixture of cis and trans X–Pro peptide bonds, since the barrier to rotation about peptide bonds results in conformational ensembles that interconvert slowly on the ^{1}H NMR time scale. It should be recognized, however, that heterogeneity of the tyrosine and histidine resonances may also be due to barriers to conformational transitions other than cis/trans isomerism if such barriers result in conformational subpopulations with lifetimes significantly longer than 1 ms.

In O-T-16, there are two prolines and therefore at least four possible conformational ensembles which can be detected by ^{1}H NMR. The splitting pattern of the Tyr C$^\epsilon$H resonances of O-T-16 in water reveals at least three conformational states (viz., *xy*, *xx*, and *yx*). The *xx*/*yx* equilibrium is also monitored by the His^{119} C$^\epsilon$H proton resonance. Because there are three (rather than two) conformational ensembles detected by the Tyr C$^\epsilon$H proton resonances, it is not possible to provide a reliable identification of those with particular (cis or trans) peptide-bond conformations by using the correlations proposed elsewhere for the Tyr C$^\epsilon$H resonances of Ac-Asn-Pro-Tyr-NHMe (Stimson et al., 1982). One can conclude only that, if *cis/trans*-proline conformational heterogeneity is present in O-T-16, it is detected by the Tyr C$^\epsilon$H and C$^\delta$H proton resonances.

The *yx*:*xx* and *xy*:*xx* ratios can be varied by titration with Me_2SO. In aqueous solutions containing greater than 50% Me_2SO, only the *xx* conformational ensemble is observed (Figure 7). Hence, no X–Pro peptide bond conformational heterogeneity is present at Me_2SO concentrations greater than 50%. This result is consistent with the fact that, in Me_2SO, Ac-Asn-Pro-Tyr-NHMe and Ac-Asn-Pro-Tyr-Val-Pro-NHMe have exclusively trans X–Pro peptide bond conformations (Stimson et al., 1986). For O-T-16, however, we cannot reliably identify which X–Pro peptide bond conformers are preferentially stabilized in ≥50% Me_2SO/water solutions.

Local Conformations of O-T-16 Affecting the Fluorescence of Tyr^{115}. Fluorescence lifetime and steady-state fluorescence measurements on Ac-Pro-Tyr-NHMe and Ac-Asn-Pro-Tyr-NHMe reveal no tyrosine fluorescence quenching relative to Ac-Tyr-NHMe and monoexponential fluorescence decay kinetics. On the other hand, NMR studies of Ac-Asn-Pro-Tyr-NHMe (Montelione et al., 1984) indicate a significant population of intramolecular hydrogen-bonded β-bend conformers (with trans Asn–Pro peptide bonds) in water, which were detected by solute/solvent saturation transfer and NOE measurements. This hydrogen-bonded conformer does not involve interactions with the tyrosine side chain and is not detected by these fluorescence measurements. In addition, both Ac-Pro-Tyr-NHMe and Ac-Asn-Pro-Tyr-NHMe exhibit *cis/trans*-proline isomerization (Stimson et al., 1982) that also

is not detected by the fluorescence lifetime measurements. In these X-Pro-Tyr peptides, *cis/trans*-proline isomerization does not result in multiple tyrosine fluorescence lifetimes.

For the single tyrosine of O-T-16, steady-state measurements indicate the presence of significant quenching relative to Ac-Tyr-NHMe, Ac-Pro-Tyr-NHMe, or Ac-Asn-Pro-Tyr-NHMe. Time-resolved fluorescence measurements demonstrate that this quenching is due to ca. 80% of molecules with quenched (τ_2 = 1.5 ± 0.2 ns) fluorescence. The remaining ca. 20% of O-T-16 molecules exhibit long fluorescence lifetimes (τ_1 = 3.6 ± 0.5 ns) not common for tyrosine peptides, indicating a local fluorophore environment which is different from that of the shorter peptides. This fluorescence heterogeneity is not due to fluorescence contaminants since the tyrosine fluorescence emission and excitation profiles of O-T-16 are the same as those of Ac-Tyr-NHMe, Ac-Pro-Tyr-NHMe, and Ac-Asn-Pro-Tyr-NHMe. Chemical homogeneity was also confirmed by reversed-phase HPLC rechromatography. Furthermore, the equilibrium between these two (or more) conformational ensembles can be altered by titration with Me_2SO. On the other hand, the local interactions responsible for the fluorescence heterogeneity of O-T-16 are not disrupted by 6 M Gdn·HCl.

The long-lifetime component of O-T-16 probably involves local interactions which slow down the electronic deactivation processes for a distinct subgroup of these molecules. Apparently, in this subgroup the phenol fluorophore is not even quenched by interactions with adjacent peptide groups which quench the fluorescence of all the smaller Tyr peptides, including Ac-L-Tyr-NHMe. Indeed, the long-lifetime component of O-T-16 is about 10% longer than the lifetime of *p*-cresol under the same conditions. It therefore is reasonable to conclude that the two subpopulations of fluorophores represent two conformational ensembles which differ in their ensemble-averaged intramolecular interactions (Gauduchon & Wahl, 1978). The short-lifetime conformer is probably quenched by interaction(s) with a polar group in the peptide. The long-lifetime conformation(s) apparently has (have) local structure which specifically restricts quenching interactions common to all the other tyrosine peptides, resulting in a long fluorescence lifetime like that observed for free tyrosine (Gauduchon & Wahl, 1978).

In an attempt to localize the interactions that control quenching of Tyr^{115} in O-T-16, we also examined the fluorescence properties of tyrosine in Ac-Asn-Pro-Tyr-Val-Pro-NHMe. In this pentapeptide which corresponds to the tyrosine-containing segment of O-T-16, the fluorescence decay is also not monoexponential. Two fluorescence decay components were observed. The longer time component (τ_1 = 2.2 ± 0.15 ns) is common to Ac-Tyr-NHMe and to all the short Pro-Tyr peptides, while the shorter lifetime (τ_2 = 0.9 ± 0.2 ns) corresponds to a quenched component. Shorter Pro-Tyr peptides which exhibit monoexponential decay in water lack the conformation-dependent interactions which cause quenching in the pentapeptide. However, unlike O-T-16 which has a *very long* fluorescence decay component (τ_1 = 3.6 ns), the long-lifetime component of Ac-Asn-Pro-Tyr-Val-Pro-NHMe is similar to that of the smaller Pro-Tyr peptides. Hence, the interactions which reduce intramolecular quenching in O-T-16 are not present in Ac-Asn-Pro-Tyr-Val-Pro-NHMe.

Since time-resolved fluorescence measurements on Ac-Asn-Pro-Tyr-Val-Pro-NHMe indicate that there are no tyrosine fluorophore interactions that give rise to ensemble-averaged lifetimes longer than that of Ac-Tyr-NHMe, we conclude that the interactions that give rise to the long tyrosine fluorescence component in O-T-16 (τ_1 = 3.6 ± 0.5 ns) are due to or stabilized by medium-range interactions involving residues outside the Asn^{113}-Pro^{114}-Tyr^{115}-Val^{116}-Pro^{117} sequence. Medium-range interactions in O-T-16 may affect the fluorescence of Tyr^{115} by stabilizing particular local backbone conformations, resulting in a longer tyrosine excited-state lifetime. Alternatively, the residues outside the Asn^{113}-Pro^{114}-Tyr^{115}-Val^{116}-Pro^{117} sequence may themselves act to protect Tyr^{115} from efficient fluorescence quenching. In either case, the fluorescence data provide evidence for a nonrandom polypeptide conformation of O-T-16 under conditions of solvent, pH, and temperature at which the complete disulfide-intact ribonuclease molecule is fully folded. The nonrandom polypeptide conformation of O-T-16 is characterized by the long-lifetime fluorescence environment of Tyr^{115}. Interactions responsible for the quenched tyrosine fluorescence environment of O-T-16, on the other hand, appear to be present also in Ac-Asn-Pro-Tyr-Val-Pro-NHMe and therefore provide no information about the presence of medium-range intramolecular interactions in O-T-16.

Additional evidence for nonrandom structure in O-T-16 is contained in the ^1H NMR spectra at pH* 3.0, 25 °C, in which it was observed that both His^{119} and Tyr^{115} aromatic side-chain chemical shifts are sensitive to the same solvent-dependent *xx/yx* conformational equilibrium. This result suggests a strong conformational correlation between these two side chains, which are separated by seven backbone and four side chain variable dihedral angles. This result indicates a high *conformational correlation length* in the Tyr^{115}-Val^{116}-Pro^{117}-Val^{118}-His^{119} sequence of the *xx* and/or the *yx* conformation ensembles.

These results demonstrate that the short- and medium-range interactions present in this 20-residue fragment, O-T-16, are sufficient to define nonrandom polypeptide conformations, even in 6 M Gdn·HCl. Such conformations could potentially play a role as polypeptide chain-folding initiation structures. It should be recognized, however, that the identification of local structures in polypeptide fragments under equilibrium folding conditions does not necessarily imply that such structures play a role in the protein folding mechanism. This is because equilibrium studies alone do not provide direct information about structures that are formed with lowest activation free energy and lie on the folding pathway. Such information can be obtained only from kinetic folding studies.

In this regard, it is interesting to cite a recent kinetic folding study (Schmid & Blascheck, 1984) in which is was found that the primary pepsin cleavage site of ribonuclease A at Phe^{120}-Asp^{121} (within the O-T-16 sequence) becomes inaccessible early in the refolding process. These kinetic data indicate that the carboxyl-terminal region of the polypeptide chain is significantly ordered in early forming kinetic folding intermediates (Schmid & Blascheck, 1984). From the existing experimental data, however, a relationship between the ordered conformation of the C-terminal region of the folding intermediate detected in kinetic refolding measurements (Schmid & Blascheck, 1984) and the nonrandom conformations of O-T-16 identified in this study by fluorescence lifetime and ^1H NMR measurements has not yet been established.

Detection of Tyr-Pro cis/trans Isomerization by Fluorescence-Detected Unfolding Experiments. Guanidine-denatured, urea-denatured, or thermally denatured, disulfide-intact ribonuclease A is an equilibrium mixture of fast- and slow-folding species (Tsong et al., 1972; Garel & Baldwin, 1975; Schmid & Baldwin, 1978; Lin & Brandts, 1983a; Mui et al., 1985). This kinetic heterogeneity has been attributed, in part,

to slow proline cis/trans peptide bond isomerization (Brandts et al., 1975; Lin & Brandts, 1983b), although other kinetic barriers may be involved (Mui et al., 1985). The interconversion between fast-folding (U_F) and slow-folding (U_S's) disulfide-intact, guanidine-denatured forms of ribonuclease A is accompanied by a change in fluorescence which can be monitored by fluorescence-detected unfolding (Rehage & Schmid, 1982). The tyrosine fluorescence of the U_S's is about 20% higher than the fluorescence of U_F. By comparing fluorescence-detected unfolding kinetics of homologous RNases from related species, Schmid et al. (1986) have shown that these fluorescence changes arise primarily from local conformational changes in the Tyr^{92}-Pro^{93}-Asn^{94} sequence, with little or no contribution from conformational changes in the Asn^{113}-Pro^{114}-Tyr^{115} sequence. In bovine ribonuclease A, this slow fluorescence-detected isomerization has kinetic properties similar to that of X–Pro cis/trans isomerization in small peptides (Rehage & Schmid, 1982; Schmid et al., 1986) and is attributed to cis/trans isomerization of the Tyr^{92}-Pro^{93} peptide bond in the conversion of U_F to U_S's. It has been proposed that the fluorescence quenching of U_F (relative to U_S's) is due to nativelike interactions between the Tyr of *cis*-Tyr^{92}-Pro^{93} and the Cys^{40}–Cys^{95} disulfide bond and/or a hydrogen bond to Lys^{37} present in the guanidine-unfolded U_F species. Phenol/disulfide interactions are known to cause phenol fluorescence quenching (Cowgill, 1967; Swadesh et al., 1987).

The physical measurements described in this study demonstrate that quenching of tyrosine in the sequence Ac-Tyr-Pro-Asn-NHMe (corresponding to the sequence Tyr^{92}-Pro^{93}-Asn-^{94} in ribonuclease A) will result in significant changes in steady-state fluorescence as the cis/trans Tyr–Pro peptide-bond equilibrium is shifted, either because the cis Tyr–Pro peptide-bond conformers are quenched or because there is a quenched trans conformational ensemble whose population is coupled to the cis/trans equilibrium. Although interactions between Tyr^{92} and the Cys^{40}–Cys^{95} disulfide bond and/or Lys^{37} may be present in U_F, the short-range interactions in Tyr-Pro-Asn also contribute to the fluorescence quenching of Tyr^{92}. More generally, the results indicate that cis/trans isomerization of Tyr–Pro peptide bonds subsequent to solvent denaturation will be accompanied by slow changes in the quantum yield of tyrosine. These fluorescence changes, which monitor the isomerization process, should be generally observable for Tyr-Pro sequences in polypeptides and proteins.

ACKNOWLEDGMENTS

We thank Y. C. Meinwald and E. R. Stimson for providing several of the peptides used in this study, T. W. Thannhauser for the amino acid analyses, and R. August and M. Maytal for technical assistance.

REFERENCES

Berlman, I. B. (1976) *Handbook of Fluorescence Spectra of Aromatic Molecules*, p 123, Academic Press, New York.
Bierzynski, A., Kim, P. S., & Baldwin, R. L. (1982) *Proc. Natl. Acad. Sci. U.S.A. 79*, 2470.
Brandts, J. F., Halvorson, H. R., & Brennan, M. (1975) *Biochemistry 14*, 4953.
Brown, J. E., & Klee, W. A. (1971) *Biochemistry 10*, 470.
Chavez, L. G., Jr., & Scheraga, H. A. (1980) *Biochemistry 19*, 1005.
Cowgill, R. W. (1967) *Biochim. Biophys. Acta 140*, 37.
Ferrige, A. G., & Lindon, J. C. (1978) *J. Magn. Reson. 31*, 337.
Galat, A., Creighton, T. E., Lord, R. C., & Blout, E. R. (1981) *Biochemistry 20*, 594.
Garel, J.-R., & Baldwin, R. L. (1975) *J. Mol. Biol. 94*, 611.
Gauduchon, P., & Wahl, P. (1978) *Biophys. Chem. 8*, 87.
Gō, N., & Abe, H. (1981) *Biopolymers 20*, 991.
Grinvald, A., & Steinberg, I. Z. (1974) *Anal. Biochem. 59*, 583.
Haas, E., Wilchek, M., Katchalski-Katzir, E., & Steinberg, I. Z. (1975) *Proc. Natl. Acad. Sci. U.S.A. 72*, 1807.
Hazan, G. (1973) Ph.D. Thesis, Feinberg Graduate School, Weizmann Institute of Science.
Hazan, G., Grinvald, A., Maytal, M., & Steinberg, I. Z. (1974) *Rev. Sci. Instrum. 45*, 1602.
Hirs, C. H. W. (1956) *J. Biol. Chem. 219*, 611.
Hirs, C. H. W., Moore, S., & Stein, W. H. (1956) *J. Biol. Chem. 219*, 623.
Hundley, L., Coburn, T., Garwin, E., & Stryer, L. (1967) *Rev. Sci. Instrum. 38*, 488.
Karplus, M., & Weaver, D. L. (1976) *Nature (London) 260*, 404.
Kim, P. S., & Baldwin, R. L. (1982) *Annu. Rev. Biochem. 51*, 459.
Konishi, Y., Ooi, T., & Scheraga, H. A. (1982) *Proc. Natl. Acad. Sci. U.S.A. 79*, 5734.
Kotelchuck, D., & Scheraga, H. A. (1968) *Proc. Natl. Acad. Sci. U.S.A. 61*, 1163.
Kunimitsu, D. K., Woody, A. Y., Stimson, E. R., & Scheraga, H. A. (1968) *J. Phys. Chem. 72*, 856.
Lin, L.-N., & Brandts, J. F. (1983a) *Biochemistry 22*, 564.
Lin, L.-N., & Brandts, J. F. (1983b) *Biochemistry 22*, 559.
Lord, R. C., & Relyea, N. M. (1981) *J. Raman Spectrosc. 11*, 315.
Lynn, R. M., Konishi, Y., & Scheraga, H. A. (1984) *Biochemistry 23*, 2470.
Marion, D., & Wüthrich, K. (1983) *Biochem. Biophys. Res. Commun. 113*, 967.
Markley, J. L. (1975) *Biochemistry 14*, 3546.
Marquardt, D. W. (1963) *J. Soc. Ind. Appl. Math. 11*, 431.
Matheson, R. R., Jr., & Scheraga, H. A. (1978) *Macromolecules 11*, 819.
McWherter, C. A., Thannhauser, T. W., Fredrickson, R. A., Zagotta, M. T., & Scheraga, H. A. (1984) *Anal. Biochem. 141*, 523.
Montelione, G. T., Arnold, E., Meinwald, Y. C., Stimson, E. R., Denton, J. B., Huang, S.-G., Clardy, J., & Scheraga, H. A. (1984) *J. Am. Chem. Soc. 106*, 7946.
Mui, P. W., Konishi, Y., & Scheraga, H. A. (1985) *Biochemistry 24*, 4481.
Némethy, G., & Scheraga, H. A. (1979) *Proc. Natl. Acad. Sci. U.S.A. 76*, 6050.
Oka, M., Montelione, G. T., & Scheraga, H. A. (1984) *J. Am. Chem. Soc. 106*, 7959.
Piantini, U., Sørensen, O. W., & Ernst, R. R. (1982) *J. Am. Chem. Soc. 104*, 6800.
Pincus, M. R., Gerewitz, F., Wako, H., & Scheraga, H. A. (1983) *J. Protein Chem. 2*, 131.
Ptitsyn, O. B. (1973) *Akad. Nauk SSSR, Dokl. Biophys. 210*, 87.
Rayner, D. M., & Szabo, A. G. (1978) *Can. J. Chem. 56*, 743.
Redfield, A. G., & Kunz, S. D. (1975) *J. Magn. Reson. 19*, 250.
Rehage, A., & Schmid, F. X. (1982) *Biochemistry 21*, 1499.
Schaffer, S. W. (1975) *Int. J. Pept. Protein Res. 7*, 179.
Scheraga, H. A. (1973) *Pure Appl. Chem. 36*, 1.

Scheraga, H. A. (1985) *Proc. Natl. Acad. Sci. U.S.A. 82*, 5585.
Schimmel, P. R., & Flory, P. J. (1968) *J. Mol. Biol. 34*, 105.
Schmid, F. X., & Baldwin, R. L. (1978) *Proc. Natl. Acad. Sci. U.S.A. 75*, 4764.
Schmid, F. X., & Blaschek, H. (1984) *Biochemistry 23*, 2128.
Schmid, F. X., Grafl, R., Wrba, A., & Beintema, J. J. (1986) *Proc. Natl. Acad. Sci. U.S.A. 83*, 872.
Shoemaker, K. R., Kim, P. S., Brems, D. N., Marqusee, S., York, E. J., Chaiken, I. M., Stewart, J. M., & Baldwin, R. L. (1985) *Proc. Natl. Acad. Sci. U.S.A. 82*, 2349.
Silverman, D. N., Kotelchuck, D., Taylor, G. T., & Scheraga, H. A. (1972) *Arch. Biochem. Biophys. 150*, 757.
Stimson, E. R., Montelione, G. T., Meinwald, Y. C., Rudolph, R. K. E., & Scheraga, H. A. (1982) *Biochemistry 21*, 5252.
Stimson, E. R., Meinwald, Y. C., Montelione, G. T., & Scheraga, H. A. (1986) *Int. J. Pept. Protein Res. 27*, 569.
Swadesh, J. K., Montelione, G. T., Thannhauser, T. W., & Scheraga, H. A. (1984) *Proc. Natl. Acad. Sci. U.S.A. 81*, 4606.
Swadesh, J. K., Mui, P. W., & Scheraga, H. A. (1987) *Biochemistry* (submitted for publication).
Takahashi, S., Kontani, T., Yoneda, M., & Ooi, T. (1977) *J. Biochem. (Tokyo) 82*, 1127.
Tanaka, S., & Scheraga, H. A. (1975) *Proc. Natl. Acad. Sci. U.S.A. 72*, 3802.
Tanaka, S., & Scheraga, H. A. (1977) *Macromolecules 10*, 291.
Tsong, T. Y., Baldwin, R. L., & Elson, E. L. (1972) *Proc. Natl. Acad. Sci. U.S.A. 69*, 1809.
VanEs, W. L., & Wisse, J. H. (1963) *Anal. Biochem. 6*, 135.
Wetlaufer, D. B. (1973) *Proc. Natl. Acad. Sci. U.S.A. 70*, 697.
Zimmerman, S. S., & Scheraga, H. A. (1977) *Biopolymers 16*, 811.

Definitive Characterization of Human Thymine Glycol *N*-Glycosylase Activity†

Susan A. Higgins,‡ Krystyna Frenkel,‡ Archie Cummings,§ and George W. Teebor*,§
Departments of Environmental Medicine and Pathology, New York University Medical Center, New York, New York 10016
Received July 25, 1986; Revised Manuscript Received November 14, 1986

ABSTRACT: An *N*-glycosylase activity that released *cis*-[^{3}H]-5,6-dihydroxy-5,6-dihydrothymine (thymine glycol, TG) from chemically oxidized poly(dA-[^{3}H]dT) was unambiguously characterized both in extracts of HeLa cells and in purified *Escherichia coli* endonuclease III. This was accomplished by use of a microderivatization procedure that quantitatively converted *cis*-TG to 5-hydroxy-5-methylhydantoin (HMH). The reaction products were analyzed by high-pressure liquid chromatography before and after derivatization by using *cis*-[^{14}C]TG and [^{14}C]HMH, which had been independently synthesized, as reference compounds. This technique facilitated construction of a $v/[E]_t$ plot for the enzyme activity in HeLa cells, permitting estimation of its specific activity. The results obtained prove the existence of both human and bacterial *N*-glycosylase activities that effect removal of TG from DNA.

Thymine is the most susceptible of the DNA bases to modification by chemical oxidants (Iida & Hayatsu, 1971), oxygen-containing free radicals (Cadet & Teoule, 1978), and ionizing radiation (Scholes, 1976). The oxidative derivative that is most readily formed is the *cis*-5,6-dihydroxy-5,6-dihydrothymine (thymine glycol, TG)[1] moiety (Teoule et al., 1977). Thymine glycol has also been identified in DNA exposed to a variety of oxidative stresses (Hariharran & Cerutti, 1977; Frenkel et al., 1981a,b, 1986; Teebor et al., 1982a), where it has been shown to be a block to DNA replication in vitro (Ide et al., 1985; Rouet & Essigman, 1985). Thymine glycol is removed from DNA through the action of an *N*-glycosylase activity of *Escherichia coli* endonuclease III (Demple & Linn, 1980; Breimer & Lindahl, 1984). Its disappearance from the DNA of mammalian cells was first described in cell culture by Mattern et al. (1973). More recently, Cathcart et al. (1984) detected TG in both rodent and human urine and concluded that this was evidence of its ongoing formation in cellular DNA through endogenous oxidation and its removal by a repair enzyme. Yet, surprisingly, TG *N*-glycosylase activity has been difficult to characterize with certainty in mammalian cells. Breimer (1983) could not detect release of TG from an oxidized copolymer of dA and dT residues by an extract of calf thymus tissue. However, when the TG moieties were converted to urea residues, the enzymatic release of urea was easily detected. Only after partial purification of the urea *N*-glycosylase could Breimer detect TG release, and then it was at a rate less than 1% that of urea. Doetsch et al. (1986) described release of ^{3}H-labeled material from an oxidized poly(dA-[^{3}H]dT) substrate by calf thymus extracts. High-pressure liquid chromatographic (HPLC) analysis of the material showed the presence of three peaks, one of which eluted with the retention time of TG. The nature of the other two was not certain.

To definitively characterize this important enzyme activity, we devised a facile microderivatization scheme based on the work of Teoule et al. (1974) and modified by us for HPLC (Frenkel et al., 1982). This technique unambiguously and

† This work was supported by USPHS Grants CA 16669 and ES 07081. A portion of this work was presented at the meeting of the American Association for Cancer Research, Los Angeles, CA, May 7–10, 1986 (Higgins et al., 1986).
* Author to whom correspondence should be addressed.
‡ Department of Environmental Medicine.
§ Department of Pathology.

[1] Abbreviations: TG, thymine glycol (5,6-dihydroxy-5,6-dihydrothymine); dTG, thymidine glycol (5,6-dihydroxy-5,6-dihydrothymidine); HMH, 5-hydroxy-5-methylhydantoin; dT, thymidine; EDTA, disodium ethylenediaminetetraacetate; DTT, dithiothreitol; Tris, tris(hydroxymethyl)aminomethane; BE buffer, 100 mM NaCl, 20 mM Tris-HCl, and 1 mM EDTA, pH 7.5; HPLC, high-pressure liquid chromatography; ODS, octadecylsilane; HAP, hydroxylapatite.

0006-2960/87/0426-1683$01.50/0